Shape Similarity based Surface Registration

Manuel Frei and Simon Winkelbach
Institute for Robotics and Process Control, TU Braunschweig, Muehlenpfordtstr. 23, Braunschweig, Germany

Keywords: Surface Registration, Scan Alignment, Self-similarity, Surface-based Feature, RANSAC, RANSAM, 3D Puzzle.

Abstract: In the last 20 years many approaches for the registration and localization of surfaces were developed. Most of them generate solutions by minimizing point distances or maximizing contact areas between surface points. Other algorithms try to detect corresponding points on the two surfaces by searching for points with same features and align them. However, aligning and localizing self-similar surfaces or surfaces having large regions with approximately constant curvature is still a complex problem.
In this paper a new algorithm for registration and matching of surfaces is introduced, which extends an approach maximizing the contact area between the surfaces by surface-based dissimilarity features and thereby solves the problem of registering the problematic surfaces described above.
Our evaluation shows the great potential of our approach regarding efficiency, accuracy and robustness for various applications like scan alignment, pottery assembly or bone reduction.

1 INTRODUCTION

Matching and registration of surfaces is an important problem for many applications. Hereby the general goal is the generation of a rigid body transformation that aligns two surfaces. The field of applications includes registration of partially overlapping surfaces or volumes, object recognition, object localization and reconstruction of broken objects like broken pottery or bone fractures in computer aided surgery. A review of all published registration algorithms would go beyond the scope of this paper. Therefore we just give a short summary of the most related work.

A standard algorithm for registration is the Iterative Closest Point (ICP) algorithm, which aligns two surfaces by iteratively searching for closest points and calculating a transformation to align them (Besl and McKay, 1992). Other ICP variants enhance the original algorithm by using additional information like texture (Papatheodorou and Rueckert, 2004), colour (Johnson and Kang, 1997) or pseudo colour attributes (Romero and Devy, 2008). However, the limitation of the ICP algorithms is that an initial pose must be known in advance.

Before performing a fine registration with ICP usually a coarse registration has to be executed to find an initial pose. Here two general procedures can be differentiated.

The first class are algorithms registering surfaces by searching for corresponding surface points with characterizing features. Points with very similar surface features probably correspond. These corresponding points can then be used for the calculation of a rigid transformation which aligns the two surfaces. In general a feature can be any characterizing property of a region or a point. They can be very complex as spin images (Johnson and Hebert, 1999) or signatures of histograms of orientations (Tombari et al., 2010) whose advantage is that there are only few points on the other surface with similar ones. Other approaches use low-dimensional surface features like surface curvatures (Yamany and Farag, 2002), edge points (Sertel and Ünsalan, 2006), 3d surface lines (Yao et al., 2010) or surface integration based features (Gelfand et al., 2005). Their advantage in respect to the complex ones is the low complexity of computing, storing and comparing. However, with decreasing feature complexity the difficulty of detecting correct point correspondences especially increases when processing surfaces being noisy or highly self-similar or having large regions with nearly constant curvature.

The approaches belonging to the second class try to find the best alignment by maximizing a quality function in the parameter space of all rigid transformations between both surfaces. By testing many parameter combinations the optimal alignment of the surfaces is generated. Whereas Hough Transform based methods vote between all possible parame-

Frei M. and Winkelbach S..
Shape Similarity based Surface Registration.
DOI: 10.5220/0004733603590366
In *Proceedings of the 9th International Conference on Computer Vision Theory and Applications* (VISAPP-2014), pages 359-366
ISBN: 978-989-758-003-1

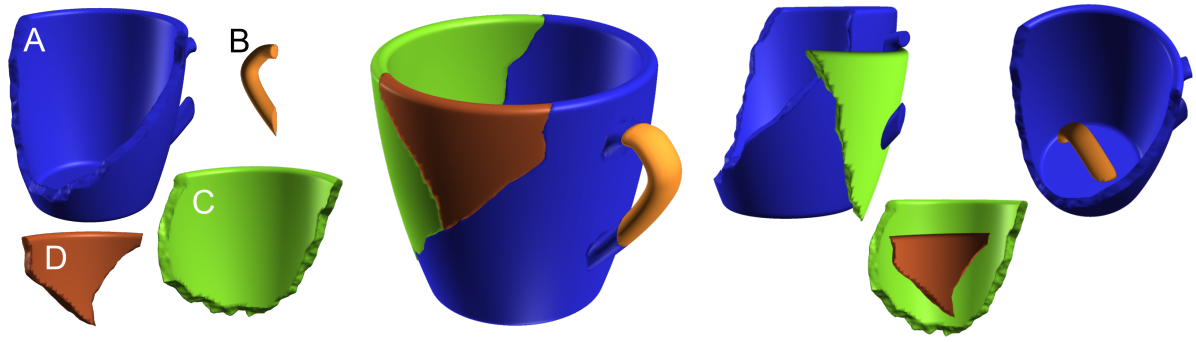

(a) (b) (c)

Figure 1: Cup fragments: (a) 4 fragments with 805 to 15721 vertices and convex hulls of 28.14 x 19.66 x 64.12 to 132.98 x 153.82 x 119.72 mm; (b) reassembled cup with eRANSAM; (c) matching results of approaches calculating the LCP.

ter combinations (Ballard, 1981), the Random Sample Consensus (RANSAC)-based approaches (Fischler and Bolles, 1981) only evaluate parameter combinations being generated by randomly selecting data points. However, because of the enormous storage consumption and the high computation times the algorithms aren't applicable without any further improvements.

Therefore (Rusu et al., 2009) introduced a RANSAC variant, Sample Consensus - Initial Alignment (SAC-IA), that reduces the number of considered surface points by detecting correspondence candidates with characterizing features (Fast Point Feature Histogram).

(Aiger et al., 2008) proposed a RANSAC variant reducing the required number of transformation hypotheses for a good solution by detecting nearly congruent coplanar 4-point sets on both surfaces.

Another RANSAC-based approach is the Random Sample Matching (RANSAM) algorithm (Winkelbach et al., 2006). It also reduces the number of required transformations compared to RANSAC by detecting congruent 2-point sets on the two surfaces with features being invariant under translation and rotation and consequently is very fast. It can be applied in many applications like the localization of objects for an industrial bin picking system (Buchholz et al., 2010), the localization of mobile robots (Iser et al., 2008), the registration of scanned surfaces (Winkelbach et al., 2006) or the reconstruction of broken objects like bone fractures (Winkelbach et al., 2004). It is robust to noise and outliers calculating the largest common point set (LCP) of two surfaces and using no surface features except surface normals. However, the registration problem of surfaces being highly self-similar or having large areas with nearly constant curvature can neither be solved by these approaches without prior knowledge of surface shape or geometry (see Figure 1 (c)).

1.1 Contribution and Overview

In this paper we present the algorithm extended Random Sample Matching (eRANSAM) which extends RANSAM by integrating a surface-based, point-wise dissimilarity feature and so combines the advantages of algorithms calculating the LCP of two surfaces and surface-based features. Thus we can handle a limitation of most registration approaches, the matching of surfaces having large regions with nearly constant curvature, no or few feature points or being highly self-similar. Since the generation of the dissimilarity feature is robust against noise the whole registration approach remains robust against noise. Another advantage of the algorithm is the fact that there is no required preprocessing on the data sets of the surfaces, like removing points or smoothing the surface.

After having applied RANSAM or eRANSAM the ICP algorithm can be used for refining the alignment results. However, all results presented in our evaluation were obtained without an ICP pose refinement.

In the following we describe the similarity feature and its generation, give an overview of the most relevant RANSAM steps and show how to extend RANSAM by the similarity feature. Finally we present some registration results of eRANSAM for various registration scenarios and compare them to those of basic RANSAM and SAC-IA.

2 INTEGRATION OF A DISSIMILARITY FEATURE INTO RANSAM

RANSAM is an efficient and robust probabilistic matching algorithm for finding a 4×4 homogeneous transformation matrix T, which aligns two surfaces (A

and B) such that the LCP of the two surfaces is computed. It is based on the well-known RANSAC approach, which is accelerated by a probabilistic birthday attack (Weisstein, 2008).

By using the birthday attack many potential pose hypotheses are generated rapidly. The subsequent evaluation of these likely poses is accelerated by a Monte Carlo approximation whereby poor transformations are dropped early.

In this section eRANSAM is introduced which combines RANSAM with a surface-based dissimilarity feature. Therefore we first present the point-wise dissimilarity feature and the calculation of the dissimilarity weights. Second, we present some important RANSAM steps, the generation of pose hypotheses and the quality estimation of transformations, and show how we can enhance them by integrating the calculated weights.

But first we define some basics. Given the sets P_A and P_B of 3D point coordinates and the sets N_A and N_B of their corresponding 3D surface normals. We define the combination of a 3D point coordinate and its corresponding surface normal in 3D as an oriented point (6D parameter vector) (Johnson and Hebert, 1997) and a pair of oriented points as a dipole. Additionally in this paper we extend the 6D parameter vector to a 7D parameter vector by adding one weight per point from the sets W_A and W_B whose generation is introduced in the following section:

$$\begin{aligned} A &:= \{\mathbf{u} = [\mathbf{p}_u, \mathbf{n}_u, w_u] \,|\mathbf{p}_u \in P_A, \mathbf{n}_u \in N_A, w_u \in W_A\}, \\ B &:= \{\mathbf{v} = [\mathbf{p}_v, \mathbf{n}_v, w_v] \,|\mathbf{p}_v \in P_B, \mathbf{n}_v \in N_B, w_v \in W_B\}. \end{aligned} \tag{1}$$

Furthermore we define the boolean contact function

$$c(T, \mathbf{a}, \mathbf{b}) = |\mathbf{p}_a - T\mathbf{p}_b| < \varepsilon_p \wedge 1 - \left|\mathbf{n}_a^T H_i \mathbf{n}_b\right| < \varepsilon_n \tag{2}$$

which evaluates if two points $\mathbf{a}$ and $\mathbf{b}$ are in contact to each other after being transformed into a common coordinate system by the transformation T. The constants ε_i represent small tolerance values for a tolerated point distance and normal deviation depending on noise and the point sampling resolution.

2.1 Dissimilarity Feature

In (Winkelbach et al., 2012) an approach for the generation of a shape-similarity rating for each surface point is introduced. This algorithm assigns high similarity values to those points or surface regions being very similar to many surface regions of a given reference shape. By simply inverting the evaluation of this approach we calculate a dissimilarity feature which is illustrated by broken cup fragments in Figure 2.

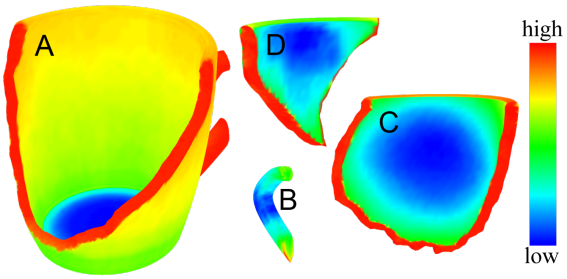

Figure 2: Illustration of the dissimilarity of the cup fragments (red represents high values, blue low values).

The algorithm consists of two steps, first generating potential alignments between source and reference shape and second calculating a dissimilarity rating depending on the generated transformations.

For the generation of a set of k potential matching hypotheses $H = \{H_1, H_2, ...H_k\}$ where H_i is a 4×4 homogeneous transformation matrix we use the RANSAM algorithm. However, any probabilistic matching algorithm can be used generating partial matches which are homogeneously distributed and fulfil some conditions like a minimum number of contact points.

In the second step for each surface point $\mathbf{a} \in A$ the subset

$$H(\mathbf{a}) = \{H_i \,|\neg\exists \mathbf{b} \in B : c(H_i, \mathbf{a}, \mathbf{b})\} \subseteq H \tag{3}$$

is calculated which is the set of all hypotheses where $\mathbf{a}$ is not in contact with the reference surface B.

Now the proportion $p(\mathbf{a}) = \frac{|H(\mathbf{a})|}{|H|}$ can be regarded as the probability that RANSAM doesn't match surface B in such a way that a point $\mathbf{a}$ is in contact with it. Thus, it can be used as a measure for dissimilarity between reference surface and the source surface.

In order to further increase the relevance of dissimilar points in the registration process we calculate dissimilarity weights

$$w_a = |H(\mathbf{a})|^2 \tag{4}$$

by squaring the dissimilarity rating. They can be calculated before executing the registration algorithm.

The runtime of registration scenarios can be reduced by ignoring points being highly self-similar using an automatically calculated threshold. We used the Otsu threshold method (Otsu, 1979) which categorizes weights into two classes such that the intra-class variance is minimized and the inter-class variance is maximized. The calculated threshold t is then used for weight calculation:

$$w_a = \begin{cases} |H(\mathbf{a})|^2 & |H(\mathbf{a})| > t, \\ 0 & otherwise \end{cases}. \tag{5}$$

A comparison of eRANSAM with and without threshold usage can be found in our evaluation.

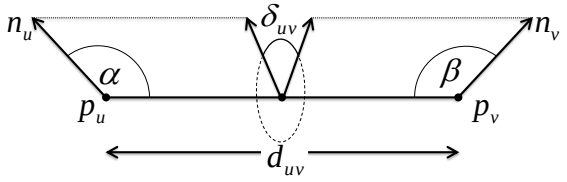

Figure 3: Geometric relations of a dipole being invariant under rotation and translation.

2.2 Rapid Generation of Likely Pose Hypotheses

RANSAM includes a very fast approach to find likely pose hypotheses by assuming a contact between A and B, e.g. a contact between dipoles. Such dipoles of A and B, which are geometrically congruent, are candidates for contact points to be aligned. Geometrical congruent means, that they have the same geometric relations

$$rel(\mathbf{u},\mathbf{v}) = (d_{uv}, \alpha, \beta, \delta_{uv})^T \quad (6)$$

(see Figure 3) where d_{uv} is the euclidean distance between point $\mathbf{p}_u$ and $\mathbf{p}_v$, α is the angle between the normal $\mathbf{n}_u$ and the line through $\mathbf{p}_u$ and $\mathbf{p}_v$, β is the angle between the normal $\mathbf{n}_v$ and the line through $\mathbf{p}_u$ and $\mathbf{p}_v$ and δ_{uv} is the angle between the normals $\mathbf{n}_u$ and $\mathbf{n}_v$ around the line through $\mathbf{p}_u$ and $\mathbf{p}_v$.
The search for congruent dipoles is accelerated by exploiting the birthday attack. Therefore two 4D relation tables (R_A and R_B) are used in which already selected dipoles are stored using $rel(\mathbf{u},\mathbf{v})$ as table indices.

Instead of selecting dipoles of A and B randomly (RANSAM) we use their weights W_A and W_B as selection probability (eRANSAM). In this way points having higher dissimilarity weights are selected more often and so relevant matching hypotheses are generated more often. This results in the following loop:

1. Select a random dipole $(\mathbf{a},\mathbf{c}) \in A$ using w_a and w_c as selection probabilities and calculate $rel(\mathbf{a},\mathbf{c})$.
2. Insert the dipole into the relation table R_A: $R_A[rel(\mathbf{a},\mathbf{c})] = (\mathbf{a},\mathbf{c})$.
3. Read out the same position of R_B: $(\mathbf{b},\mathbf{d}) = R_B[\mathrm{rel}(\mathbf{a},\mathbf{c})]$. If there is an entry the new pose hypothesis is calculated by bringing $(\mathbf{a},\mathbf{c})$ and $(\mathbf{b},\mathbf{d})$ into contact.
4. Now the same procedure is done with the other surface:
   Select a random dipole $(\mathbf{b},\mathbf{d}) \in B$ using w_b and w_d as selection probabilities and calculate $rel(\mathbf{b},\mathbf{d})$.
5. Insert the dipole into the relation table R_B: $R_B[rel(\mathbf{b},\mathbf{d})] = (\mathbf{b},\mathbf{d})$.
6. Read out the same position of R_A: $(\mathbf{a},\mathbf{c}) = R_A[\mathrm{rel}(\mathbf{b},\mathbf{d})]$. If there is an entry the new pose hypothesis is calculated by bringing $(\mathbf{a},\mathbf{c})$ and $(\mathbf{b},\mathbf{d})$ into contact.

These steps are repeated until the generated pose hypothesis satisfies a certain condition, e.g. an achieved sufficient quality or an exceeded predefined time limit.

A simple approach for calculating the relative homogeneous transformation T aligning two dipoles is given in (Winkelbach et al., 2006).

2.3 Weighted Random Sampling

As mentioned above lots of dipoles of A and B have to be selected for generating an adequate number of likely pose hypotheses. For this reason the random sampling has to be very fast. As a tradeoff between runtime and an accurate weighted random selection the following quick heuristic algorithm is used in eRANSAM where step 1 to 3 can be performed offline and only step 4 has to be executed for each weighted random sample of a point:

1. Sort the oriented points of A (B) by their weights W_A (W_B).
2. Generate $\lceil\sqrt{n}\rceil$ bins where $n = |A|$ ($n = |B|$).
3. Fill the bins consecutively with the sorted points in such a way that all bins have approximately the same sum of weights $\frac{\sum_{i=1}^{n} w_i}{\lceil\sqrt{n}\rceil}$ (first use the oriented points with the highest dissimilarity rating).
4. Select two random numbers, use the first one to select bin k ($0 \leq k \leq \lceil\sqrt{n}\rceil$) and the second one to select a random oriented point of bin k.

In this way we obtain bins containing few oriented points with high weights and bins containing lots of oriented points having smaller weights.

Alternatively any algorithm performing a weighted random sampling can be used, e.g. (Murray et al., 2013).

2.4 Quality Estimation of Likely Pose Hypotheses

The basic RANSAM algorithm estimates the quality of a likely pose hypothesis by calculating the proportion of overlapping area

$$\Omega \approx \frac{\sum_{i=1}^{n} w_B(T,\mathbf{a}_i)}{|A|}, \quad (7)$$

where $w_B(T,\mathbf{a})$ is a function which returns 1 if the oriented point $\mathbf{a} \in A$ is in contact with surface B after being transformed by T and 0 otherwise. RANSAM and

Table 1: Registration performance of 250 test runs: comparison of the RMSE in mm of corresponding vertices of the best pose, RANSAM, SAC-IA, eRANSAM and eRANSAM with an Otsu threshold at dissimilarity weight calculation (eRANSAM$_t$) for various registration scenarios.

	best pose	RANSAM			SAC-IA	eRANSAM			eRANSAM$_t$		
object (Figure)		min	med	max		min	med	max	min	med	max
cup A+B (1)	0.00	94.4	110	127	78.2	0.1	1.6	5.0	0.1	1.6	3.5
cup A+C (1)	0.00	108	117	119	52.0	0.9	3.8	116	0.7	2.9	166
cup A+D (1)	0.00	76.9	88.5	123	47.0	0.2	2.6	163	0.2	2.1	153
cup C+D (1)	0.00	61.2	92.0	106	56.2	0.0	1.5	4.9	0.0	1.4	6.2
femur (5)	0.53	26.3	41.7	59.2	22.6	0.6	1.4	3.6	0.6	1.3	3.1
cup scans (6)	0.15	66.5	76.9	86.5	25.3	0.3	0.8	3.1	0.3	0.8	3.8
cylinder (7)	0.09	8.0	9.0	9.9	5.2	0.2	0.9	2.6	0.1	1.0	17.0
plane (8)	0.03	5.9	6.0	6.0	4.6	0.4	0.4	0.7	0.4	0.4	0.7

eRANSAM accelerate these computations by using a k-d-tree to detect contact points and by performing an efficient Monte Carlo strategy to drop transformations with a weak forecasted matching quality early.

In eRANSAM we additionally use the precalculated weights to favour dissimilar points being in contact over similar ones. Therefore we use the same quality function (7) as RANSAM but we apply another w_B-function:

$$w_B(T,\mathbf{a}) = \begin{cases} w_a \cdot w_b, & \exists \mathbf{b} \in B : c(T,\mathbf{a},\mathbf{b}) \\ 0, & \text{otherwise} \end{cases}. \quad (8)$$

That's because we can interpret the weight w_a (w_b) of a point $\mathbf{a}$ ($\mathbf{b}$) as the probability of his nonexistence in the contact area between surface A and B. Therefore the resulting probability of successfully aligned points is given by the product of the probabilities of the independent events w_a and w_b.

3 EXPERIMENTAL RESULTS

We applied our registration algorithm to various 3d objects like potteries and bone fractures as well as to 3d scans and compared the generated results to those of basic RANSAM and SAC-IA. All evaluations were executed on an Intel Core 2 Quad with 2,83 GHz on one single core. The runtime of eRANSAM was between 2 and 10 seconds depending on the number of surface points of the datasets (10^4 to 10^5 points) and the corresponding weights. Weight calculation took additional 2 to 10 seconds for 100 hypotheses ($|H| = 100$). In contrast to that the runtime of SAC-IA was with 34 seconds to 8.5 minutes significantly higher.

Since eRANSAM is a probabilistic approach we performed 250 pairwise matches for each test object. The common representation for registration results is the mean error. However, it is only meaningful if the values are normally distributed. In the evaluation of eRANSAM the results aren't normally distributed and few outliers strongly influence the mean value. Hence we present the registration results as the median, the minimum and the maximum quantiles of the root mean squared error (RMSE) of correctly corresponding points of the two surfaces.

Table 1 shows the results of some evaluated registration scenarios. It illustrates that RANSAM doesn't create correct alignments for any evaluated scenario because the correct alignment doesn't coincide with the LCP of two surfaces in our scenarios. Furthermore it shows that SAC-IA neither creates correct alignments for the evaluated scenarios and additionally its registration runtime is very high. This is because there are no characterizing regions or points on the surfaces, having approximately constant curvature or being self-similar, that can be detected with the FPFH feature. So the number of surface points can't be reduced drastically and so the LCP is still not the correct registration result. Moreover, Table 1 shows that eRANSAM achieves correct and reliable results for all evaluated registration scenarios. The few presented registration results having a high RMSE are due to the limited runtime of the algorithm. If the runtime was higher, better and similar to the other solutions would be found (see also Figure 4). In this evaluation we only consider surfaces being highly self-similar or having surfaces with a nearly constant curvature and thus have a high variance in dissimilarity values. If a surface doesn't have such surface features the dissimilarity values are constant for nearly all surface points. In such a case eRANSAM achieves approximately the same registration results as basic RANSAM because no points being in contact are favoured.

3.1 3d Puzzle Problem

The characteristic of the 3d puzzle problem is the matching of 3d objects, e.g. broken ones. Most algorithms use complex segmentation techniques to detect the fractured surface or try to detect feature points (Huang et al., 2006) which is hardly possible consid-

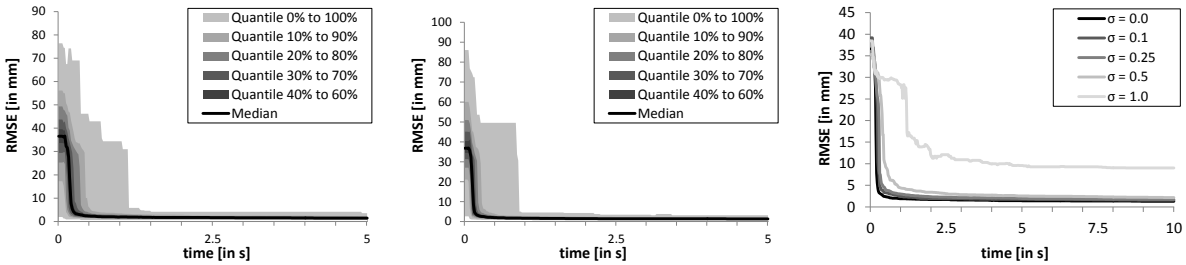

(a) (b) (c)

Figure 4: Registration error (RMSE) over time of 250 test runs: (a) median and quantiles of eRANSAM results; (b) median and quantiles of results of eRANSAM with threshold; (c) median RMSE of femur fragments with different additive noise.

Table 2: Registration results (RMSE in mm) for the femur fragments with additive noise after 5s.

	eRANSAM			eRANSAM$_t$		
femur fragments with	min	med	max	min	med	max
no noise	0.6	1.4	3.6	0.6	1.3	3.1
$\sigma = 0.1$	0.7	1.7	4.0	0.8	1.6	3.7
$\sigma = 0.25$	0.8	1.9	5.8	0.6	1.5	3.9
$\sigma = 0.5$	0.9	2.5	33.3	0.7	1.8	4.6
$\sigma = 1.0$	1.9	9.6	36.3	1.9	7.6	35.5

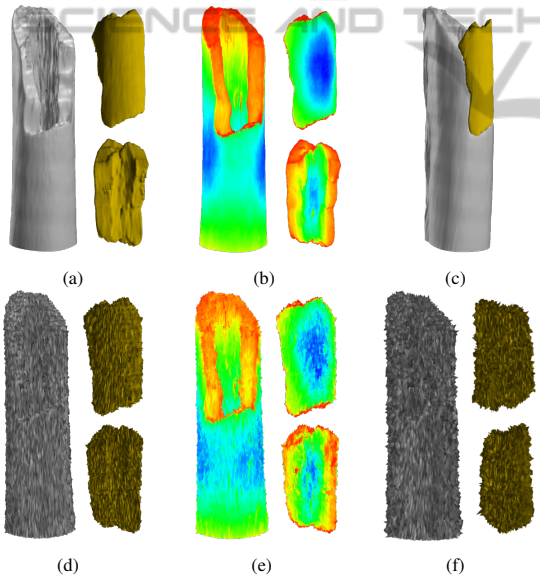

(a) (b) (c) (d) (e) (f)

Figure 5: Femur fragments: (a) Illustration of femur fragments (35822 / 9402 vertices and convex hulls of 31.42 x 106.81 x 35.76 / 23.07 x 51.59 x 18.09 mm); (b),(e) similarity (no noise/$\sigma = 0.5$); (c) matching result of eRANSAM; (d),(f) femur fragments with additive noise ($\sigma = 0.5/1.0$).

ering weathered or splintered surfaces. By applying eRANSAM we simply favour in the registration process those surface regions which are detected by the dissimilarity feature.

The femur fracture fragments (Figure 5) are reconstructed from CT data and are used for several registration scenarios. First of all, the the two fragments are matched by eRANSAM and the results are compared to those of the RANSAM and SAC-IA algorithms. While achieving wrong registration results by using basic RANSAM or SAC-IA, eRANSAM correctly aligns them. In addition to that the runtime of eRANSAM (and RANSAM) was 5 seconds and the registration runtime of SAC-IA was with 89 seconds much higher. The timing progress of eRANSAM of the distance to the correct alignment is illustrated on Figure 4 (a) and (b), where you can see that the median RMSE is below 2.5 mm already after 0.45 seconds registration time. By additionally using an Otsu threshold at dissimilarity weights calculation this registration error can already be achieved after 0.36 seconds. Table 1 also apparently shows that the usage of a threshold (e.g. Otsu) improves the registration results regarding accuracy. However it only accelerates the registration process by decreasing the number of potential selected points. Actually eRANSAM without a threshold achieves results with a higher accuracy but with a longer computation time. So the user has to decide if he rather wants to have accurate results or fast results which can be refined by ICP.

Exemplarily for all surfaces we present the performance of eRANSAM at noisy input data for the femur fragments. Therefore we apply some zero-mean Gaussian noise with various standard deviations (σ) to the surfaces. Our evaluation shows that eRANSAM is successful for surfaces with strong additive noise (see Figure 4 (c)). Even in case of the highest, evaluated noise level eRANSAM finds a solution that is good enough for a subsequent ICP optimization.

Further we applied eRANSAM to broken cup fragments and compared the results to RANSAM, SAC-IA and eRANSAM with a threshold. These

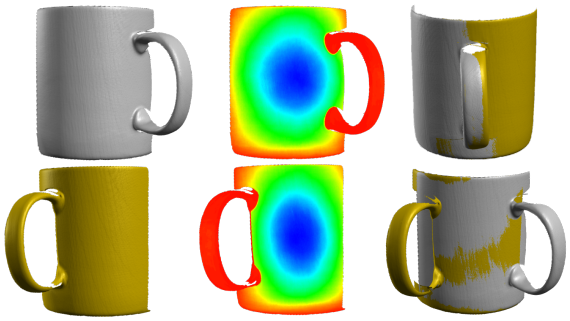

Figure 6: Illustration of cup scans (115505 / 110488 vertices and 68.04 x 94.08 x 81.03 / 57.24 x 97.58 x 91.18 mm), their similarity, an eRANSAM matching result (right top) and a wrong result with a LCP approach (right bottom).

are as well registration scenarios which could not be solved by calculating the LCP (Figure 1). As our evaluation shows, eRANSAM is able to match all fragments having a common fractured surface with a runtime of 5 seconds and so the whole broken cup can be restored. The runtime of SAC-IA achieving wrong registration results was between 32 and 65 seconds.

3.2 Scan Registration

Another application area of eRANSAM is the registration of partly overlapping scans having large regions with nearly constant curvature or being highly self-similar. Our first test object is a cup (Figure 6) which is scanned from two different viewing directions. In both scans the cup handle is visible. However, because the cup body and the cup handle have surfaces with nearly constant curvature it is difficult to detect feature points. Moreover the LCP of the two scans isn't the correct alignment either. eRANSAM can solve even this complex registration scenario since the cup handle is very dissimilar from the body and therefore receives higher dissimilarity weightings. eRANSAM isn't only faster (10 seconds) but also more accurate than SAC-IA (330 seconds).

Figure 7 illustrates another evaluated scenario for scan registration, the alignment of two surfaces of a cylinder-like object. Again the LCP approaches lead to wrong registration results with runtimes of 10 (RANSAM) and 494 seconds (SAC-IA). Although the scans don't fit together correctly because of scan deformations eRANSAM successfully aligns them with a registration time of 10 seconds.

The final presented evaluation scenario is the registration of noisy, partly overlapping planes with few dissimilar surface points (Figure 8). This is another example where eRANSAM succeeds (2.5 seconds) while LCP approaches (up to 221 seconds) fail.

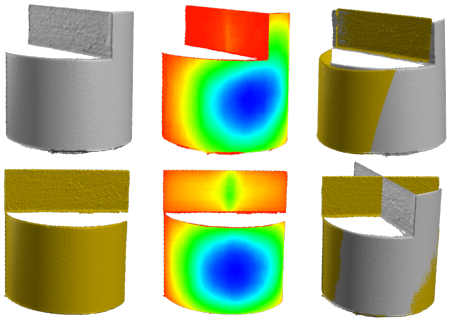

Figure 7: Illustration of scans of a cylinder-like object (50548 / 59052 vertices and 24.19 x 24.93 x 23.09 / 22.42 x 26.04 x 25.40 mm), their similarity, an eRANSAM matching result (right top) and a wrong result with a LCP approach (right bottom).

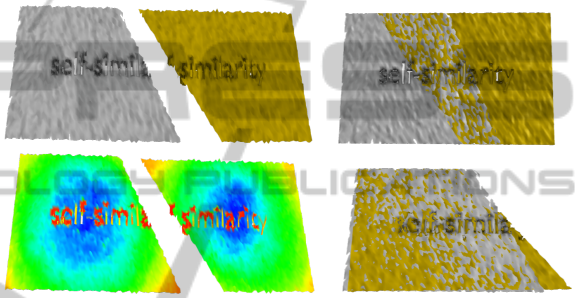

Figure 8: Illustration of planes with distinctive text (5245 / 8506 vertices and 15.05 x 2.19 x 10.00 / 16.83 x 2.18 x 10.00 mm), their similarity and an eRANSAM matching result (right top) and a wrong result with a LCP approach (right bottom).

4 CONCLUSIONS

In this paper we introduced eRANSAM, a new approach for the registration of two self-similar surfaces. Based on the RANSAM algorithm we use for the calculation of the transformation aligning the surfaces additional characterizing information which depend on a region-based dissimilarity feature. So we combine the advantages of region-based surface features and the robustness of the RANSAC-based algorithms. The dissimilarity information are integrated into RANSAM at two steps, the generation of likely pose hypotheses by selecting surface points regarding the dissimilarity and the quality estimation of likely pose hypotheses where points being in contact are weighted according to their dissimilarity values.

Our evaluation of eRANSAM achieved excellent results. Although eRANSAM doesn't require any knowledge about the surface geometry, surface shape or an initial pose it solves complex registration scenarios like registering self-similar surfaces in various

areas of application, e.g. scan alignment, reduction of bone fractures or assembly of pottery.

REFERENCES

Aiger, D., Mitra, N. J., and Cohen-Or, D. (2008). 4-points congruent sets for robust pairwise surface registration. *ACM Trans. Graph.*, 27(3):1–10.

Ballard, D. (1981). Generalizing the hough transform to detect arbitrary shapes. *Pattern Recognition*, 13(2):111 – 122.

Besl, P. and McKay, N. (1992). A method for registration of 3-d shapes. *IEEE Transactions on Pattern Analysis and Machine Intelligence*, 14(2):239–256.

Buchholz, D., Winkelbach, S., and Wahl, F. (2010). Ransam for industrial bin-picking. In *Proceedings of ISR/Robotik 2010*, pages 1–6.

Fischler, M. and Bolles, R. (1981). Random sample consensus: A paradigm for model fitting with applications to image analysis and automated cartography. *Communication of the Association for Computing Machinery*, 24(6):381–395.

Gelfand, N., Mitra, N. J., Guibas, L. J., and Pottmann, H. (2005). Robust global registration. In *Proceedings of the third Eurographics symposium on Geometry processing*.

Huang, Q.-X., Flöry, S., Gelfand, N., Hofer, M., and Pottmann, H. (2006). Reassembling fractured objects by geometric matching. *ACM Trans. Graph.*, 25(3):569–578.

Iser, R., Spehr, J., Winkelbach, S., and Wahl, F. (2008). Mobile robot localization using the fast random sample matching approach. In *Proceedings of Robotik 2008, VDI-Berichte No. 2012*, pages 163–166.

Johnson, A. and Hebert, M. (1997). Recognizing objects by matching oriented points. In *Proceedings of IEEE Conference on Computer Vision and Pattern Recognition, 1997*, pages 684–689.

Johnson, A. and Hebert, M. (1999). Using spin images for efficient object recognition in cluttered 3d scenes. *IEEE Transactions on Pattern Analysis and Machine Intelligence*, 21(5):433–449.

Johnson, A. and Kang, S. B. (1997). Registration and integration of textured 3d data. In *Proceedings of Intern. Conference on Recent Advances in 3D Digital Imaging and Modeling, 1997*, pages 234–241.

Murray, L. M., Lee, A., and Jacob, P. E. (2013). Rethinking resampling in the particle filter on graphics processing units. *ArXiv e-prints*.

Otsu, N. (1979). A threshold selection method from gray-level histograms. *IEEE Transactions on Systems, Man and Cybernetics*, 9(1):62–66.

Papatheodorou, T. and Rueckert, D. (2004). Evaluation of automatic 4d face recognition using surface and texture registration. In *Proceedings of IEEE Intern. Conference on Automatic Face and Gesture Recognition*, volume 6, pages 321–326.

Romero, F. and Devy, M. (2008). Registration by using a pseudo color attribute. In *Proceedings of Intern. Conference on Pattern Recognition*, volume 19, pages 1–4.

Rusu, R., Blodow, N., and Beetz, M. (2009). Fast point feature histograms (fpfh) for 3d registration. In *Proceedings of IEEE Intern. Conference on Robotics and Automation*, pages 3212–3217.

Sertel, O. and Ünsalan, C. (2006). Range image registration with edge detection in spherical coordinates. In *Proceedings of Intern. Conference on Multimedia Content Representation, Classification and Security*, pages 745–752.

Tombari, F., Salti, S., and Stefano, L. (2010). Unique signatures of histograms for local surface description. In *Proceedings of 11th European Conference on Computer Vision*, volume 6313, pages 356–369.

Weisstein, E. W. (2008). Birthday attack-from mathworld - a wolfram web resource[online].

Winkelbach, S., Molkenstruck, S., and Wahl, F. (2006). Low-cost laser range scanner and fast surface registration approach. *Pattern Recognition (DAGM 2006), Lecture Notes in Computer Science 4174*, pages 718–728.

Winkelbach, S., Rilk, M., Schönfelder, C., and Wahl, F. (2004). Fast random sample matching of 3d fragments. *Pattern Recognition (DAGM 2004), Lecture Notes in Computer Science 3175*, pages 129–136.

Winkelbach, S., Spehr, J., Buchholz, D., Rilk, M., and Wahl, F. (2012). Shape (self-)similarity and dissimilarity rating for segmentation and matching. In *Proceedings of Pattern Recognition (DAGM-OAGM 2012), Lecture Notes in Computer Science 7476*, pages 93–102.

Yamany, S. and Farag, A. (2002). Surface signatures: an orientation independent free-form surface representation scheme for the purpose of objects registration and matching. *IEEE Transactions on Pattern Analysis and Machine Intelligence*, 24(8):1105–1120.

Yao, J., Ruggeri, M., Taddei, P., and Sequeira, V. (2010). Robust range image registration using 3d lines. In *Proceedings of IEEE Intern. Conference on Image Processing*, volume 17, pages 4321–4324.